JAAS
Journal of Analytical Atomic Spectrometry

Accepted Manuscript

This article can be cited before page numbers have been issued, to do this please use: A. Miokovic, I. Bozicevic Mihalic, S. Fazinic and M. R. Ramos, *J. Anal. At. Spectrom.*, 2026, DOI: 10.1039/D5JA00382B.

ROYAL SOCIETY OF CHEMISTRY

rsc.li/jaas

View Article Online
DOI: 10.1039/D5JA00382B

ARTICLE

The Influence of Multiple Ionization and Chemical Effects on Magnesium Kα X-Ray Spectra in High-Resolution Proton and Alpha PIXE Measurements

Received 00th January 20xx,
Accepted 00th January 20xx

DOI: 10.1039/x0xx00000x

Anja Mioković*[a], Iva Božičević Mihalić [a], Stjepko Fazinić [a] and Mauricio Rodriguez Ramos[a]†

High-resolution wavelength-dispersive (WD) X-ray emission spectra of the Mg Kα band were measured for metallic Mg and selected Mg compounds under excitation with 2–3 MeV proton (H) and 1.5–5 MeV alpha (He) ion beams. The study investigated the influence of chemical state as well as ion beam type and energy on the positions and relative intensities of Mg Kα spectral line components. In addition to the characteristic X-ray emission line, H-induced spectra revealed KL^1 multiple ionization satellite (MIS) lines, while He excitation produced both KL^1 and KL^2 MIS groups with strong energy-dependent relative intensities. Small but measurable peaks' energy shifts were observed among different Mg compounds. Statistically significant variations in the relative intensities of KL^1 group's components, correlating with chemical bonding, were also detected. The use of He excitation resulted in enhanced sensitivity for chemical speciation.

Introduction

Particle-Induced X-ray Emission (PIXE) spectroscopy is a widely used Ion Beam Analysis (IBA) technique for determining elemental compositions in materials.[1,2] PIXE is typically performed simultaneously with other IBA techniques, such as Rutherford Backscattering Spectrometry (RBS), Particle-Induced Gamma-ray Emission (PIGE) spectroscopy, and Nuclear Reaction Analysis (NRA). When performed with focused MeV ion beams, micro-PIXE spectrometry, used alongside these other techniques, serves as a powerful tool for studying the distribution of major, minor, and trace elements in micro-samples with micron-level spatial resolution.[3]

Most PIXE experiments are conducted using proton (H) ion beams in the 2-3 MeV energy range. Typically, RBS spectra are recorded simultaneously to help identify matrix elements within a sample. RBS is commonly carried out with alpha (He) ion beams in the 0.5-3 MeV energy range. He-induced PIXE offers several advantages over the H-induced PIXE, such as a reduced secondary electron background and a lower energy threshold for this background.[4] Consequently, simultaneous use of PIXE and RBS with He ion beams is a highly attractive approach, as it yields more comprehensive data than either method used independently.[5]

Characteristic X-rays in PIXE experiments are commonly recorded with energy-dispersive (ED) silicon drift detectors (SDDs). The energy resolution of such conventional Si detectors ranges from FWHM≈80 eV for Mg K to FWHM≈120 eV for Mn Kα. Analysis of ED PIXE spectra is usually performed using dedicated software packages such as GUPIXWIN[6], which is based on the fundamental parameter approach. Accurate analysis requires careful energy calibration of the measured spectra.

Specific distortions have been reported in ED PIXE spectra of geological standards, especially in the low-energy region, when measured with SDD detectors, complicating proper energy calibration.[7] Moreover, PIXE spectra include satellite peaks arising from multiple ionization of target atoms. In the case of K-shell X-ray excitation, one or more L-shell vacancies may also be created, resulting in multiple ionization satellites (MISs), denoted KL^i, where the K vacancy is accompanied by i L vacancies. These satellites appear at slightly higher energies than their parent K lines and further distort the measured ED spectra.

The MIS effect is more pronounced for He excitation. However, its influence on the shape of K X-ray lines in lighter elements, such as Na, Mg, and Al, is non-negligible even with H ion beams. Therefore, both detector-related distortions and multiple ionization effects must be accounted for in spectral analysis.

Recently, we investigated the impact of multiple ionization K X-ray satellites on the accuracy of He-induced PIXE spectra.[5] For that purpose, high-resolution wavelength-dispersive (WD) PIXE spectra were measured for elements ranging from Mg to Cr, using pure elemental samples and their compounds. Properly designed WD spectrometers may provide high energy resolution comparable to natural X-ray line widths.

Furthermore, it is well known that X-ray spectra are sensitive to chemical effects. When measured using high-resolution spectrometers, K X-ray spectra reveal clearly resolved MIS lines and chemically induced satellite peaks, which cannot be reliably studied with a conventional ED X-rays spectrometer.

Quantitative data on relative intensities and energy shifts of individual components within the Kα and Kβ bands are

[a] Ruđer Bošković Institute, 10000 Zagreb, Croatia.
† Present Addres: Centro Nacional de Aceleradores (U. Sevilla, CSIC, J. de Andalucia), 41092 Seville, Spain

View Article Online
DOI: 10.1039/D5JA00392B

therefore valuable for assessing the impact of MIS lines on PIXE accuracy, as well as for conducting chemical speciation studies. Although Kβ lines are more sensitive to chemical effects, their intensities relative to Kα are quite low for low-Z elements such as Mg. In particular, the relative intensity of Mg Kβ to Kα is only 1.4%.[8] This is why investigating Kα chemical effects in low-Z elements is particularly important.

For this purpose, we recently measured high-resolution WD Kα X-ray emission spectra induced by 2 MeV H and 3 MeV He ions in Al metal and four Al compounds.[9] The results demonstrated that PIXE, when performed with a WD X-ray spectrometer of sufficient energy resolution, can efficiently explore chemical effects through the Kα emission band. The work also contributed to the development of a more extensive and accurate database required for improving the fitting and interpretation of H- and He-induced ED X-ray spectra in PIXE analysis software. Building such a database necessitates experimental data across various H and He ion energies and a broad range of elements.

Our focus is shifted now to even lower-Z elements, such as Na and Mg, as their Kα X-ray production cross sections can exceed that of Al. This suggests that the influence of MIS and chemical satellite lines may be even more significant for Na and Mg, offering new opportunities for chemical analysis via X-ray spectroscopy. In the present study, we aimed to measure high-resolution spectra of the Mg Kα X-ray emission band using selected Mg compounds excited by H and He ions at a few selected energies.

Experiment and analysis

The high-resolution PIXE measurements were performed using a modular end-station equipped with a WD X-ray spectrometer, developed for use with focused MeV ion beams at the Tandem Accelerator Facility of the Ruđer Bošković Institute.[10] The main components of the spectrometer include a motorized sample holder, a flat diffraction crystal, and a charged-coupled device (CCD) X-ray camera. When an ion beam, focused to approximately 10 μm in diameter, strikes the target, the emitted X-rays are diffracted by the crystal and directed toward the CCD, where two-dimensional signal images are recorded. A detailed explanation of the spectrometer's working principle and the conversion of CCD images into X-ray spectrum can be found elsewhere.[11,12]

The accessible energy window, and consequently the energy resolution, depend on the element being analyzed and the crystal being used. For measurements of Mg Kα emission band, two different crystals were used: Beryl (1010), with twice the lattice spacing 2d=15.954 Å, which provided an energy window of ΔE≈150 eV and relative resolution of FWHM(E)/E≈$9.5\cdot10^{-4}$ and ADP (101), with 2d=10.64 Å, which provided an energy window of ΔE≈40 eV and relative resolution of FWHM(E)/E≈$5.6\cdot10^{-4}$.

Compressed pellets made up of high-purity powders were used as irradiation targets. To investigate chemical effects in X-ray emission spectra, the following materials were irradiated across three separate measurement sets: Mg, Mg_2Si, Mg_3N_2, MgB_2, $MgBr_2$, MgO, $MgSO_4$, and $MgWO_4$. In the first set, mixtures of all materials with Ge powder were irradiated with a 2 MeV H beam. In the second and third sets, all materials were irradiated with 2 MeV H and 3 MeV He beams. To examine the influence of varying ion beam energies on X-ray emission, two additional measurement sets were performed. In the fourth set, Mg and MgO targets were irradiated with H ions at 2.5 MeV and 3 MeV. In the fifth set, the Mg target was irradiated with He ions at 1.5 MeV, 4 MeV, and 5 MeV. A summary of all measurements is provided in Table 1. In all cases, the ion beam current was maintained between 1 and 3 nA.

Table 1. Summary of all performed measurements. × presents measurement performed on pure target. ^{Ge}× presents measurement performed on target mixed with Ge.

Irradiation		Targets							
Ion beam	Energy (MeV)	Mg	Mg_2Si	Mg_3N_2	MgB_2	$MgBr_2$	MgO	$MgSO_4$	$MgWO_4$
H	2	^{Ge}××	^{Ge}××	^{Ge}××	^{Ge}××	^{Ge}××	^{Ge}××	^{Ge}××	^{Ge}××
	2.5	×					×		
	3	×					×		
He	1.5	×							
	3	×	×	×	×	×	×	×	×
	4	×							
	5	×							

The first measurement set was required to perform energy calibration of measured spectra. A straightforward equation relates the CCD channel, where a diffracted X-ray is detected, to the energy of that X-ray. The equation is given in Ref.[10] as Eq. 1 and it shows that two known energy-channel pairs are necessary to perform energy calibration. Mg Kα components span the energy range of 1250-1290 eV. The tabulated X-ray energies reported by Deslattes et al.[13] were inspected and the Ge Lα and Ge Lβ peaks, located at 1188.01 eV and 1218.5 eV, were identified as the most suitable reference lines for the energy calibration. These lines served as internal standard for all Mg compounds. Using Beryl (1010) as the diffraction crystal provided a sufficiently wide energy window to record both Ge L lines and Mg Kα lines of interest in the same spectrum. All the other measurements, focused solely on detecting Mg Kα components with the highest possible resolution, were performed using the ADP (101) crystal.

The energy calibration procedure began with the spectrum of the Mg and Ge mixture, shown in Figure 1. Experimental X-ray energies reported by Deslattes et al.[13] were assigned to channel centroids (defined in the following paragraph) of the two most prominent peaks – Ge Lα at 1188.01 eV and Mg $K\alpha_{1,2}$ at 1253.604 eV. Using these two reference points, the energy of the Ge Lβ peak was calculated via the energy-calibration equation. The known energies of the two Ge L peaks were then used to determine the Mg $K\alpha_{1,2}$ and Mg $K\alpha_3$ energies in all other spectra of Mg compounds and Ge mixtures. Finally, these calculated energies were paired with the corresponding channel centroids in all measured spectra of pure Mg compounds, enabling the determination of energies for all other resolved X-ray peaks.

Journal Name ARTICLE

View Article Online
DOI: 10.1039/D5JA00383B

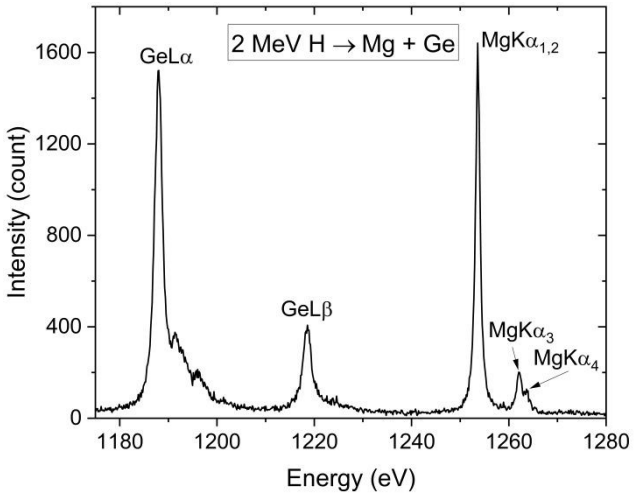

Figure 1. Measured X-ray emission spectrum of the Mg and Ge mixture excited by 2 MeV H used for energy calibration.

It is worth mentioning the higher-energy satellite lines (Lα′, Lα′′ and Lα′′′) accompanying the Ge Lα characteristic line present in Figure 1. For an atom with a singly ionized L_3 state, a transition from $M_{4,5}$ to L_3 state contributes to the Lα main line. If an atom is in a doubly ionized state, with an electron missing from both L_3 and one of the five M subshells, higher-energy satellite lines are emitted.[14] While the positions of these MIS lines do not depend on the excitation source, their relative intensities are influenced by ion beam energy and type. Selecting the H ion beam rather than the He ion beam for energy calibration ensured that intensities of the Ge Lα MIS lines were sufficiently low and did not distort the characteristic Ge Lα line, thereby preventing calibration errors.

The channel centroids of the peaks were calculated using the formula:

$$Centroid = \sum_{ch} ch \cdot I_{ch} / \sum_{ch} I_{ch}$$

where ch denotes the channel number and I_{ch} the corresponding intensity. It is worth noting that the uncertainty of each centroid can be straightforwardly determined by propagating the Poisson uncertainty of the counts in each channel. Different choices can be made for defining the upper and lower channel limits around the peak maximum in the centroid calculation. A common approach is to include intensities down to a specific percentage of a peak maximum.[15] However, we observed significant variations in the calculated centroid depending on the percentage of maximum intensity used to define these limits. Therefore, when possible, we avoided relying on a single percentage threshold. Instead, the most probable centroid was calculated as the average of the centroids obtained over a range of threshold values. Specifically, we used all intensity thresholds starting from the lowest one that clearly exceeds the background and excludes neighbouring peak regions, up to 60% of the peak maximum, in increments of 5%. For well-defined Mg $K\alpha_{1,2}$ peaks, the lower threshold reached as low as 20%. However, for less well-resolved peaks, such as Mg $K\alpha_3$ in spectra of Mg compounds and Ge mixtures, as well as Mg $K\alpha_4$, $K\alpha_5$, and $K\alpha_6$ in the remaining spectra, a fixed threshold of 60% had to be used.

Peaks' energy uncertainties were estimated using Monte Carlo-based uncertainty propagation. For each known energy-channel pair, new samples were drawn from a Gaussian distribution, with means defined by the original centroids and energies, and standard deviations equal to their respective uncertainties. The energy-calibration equation was solved for every sampled pair, generating a distribution of calculated energies. The energy uncertainty was then determined as the standard deviation of this resulting distribution.

Besides energy calibration, the measured spectra were subjected to intensity correction. There are three reasons why the raw intensity data requires adjustment. First, the above-described energy calibration involves a transformation of the intensity scale, as described in Ref[16]. Second, the intensity must be corrected for the variation in the solid angle that covers each CCD channel. Third, the intensity correction should account for the energy dependence of X-ray transmission through a 2 µm graphite-coated Mylar foil, which is placed in front of the CCD to eliminate the possible influence of ion-beam-induced luminescence. Together with energy calibration, these intensity corrections ensure that the final spectra precisely reflect the physical X-ray emission characteristics.

In order to accurately inspect intensities of all peaks' components, the spectra from pure Mg and its compounds recorded using the ADP (101) diffraction crystal were fitted, as demonstrated in Figure 2. Each resolved peak was modelled

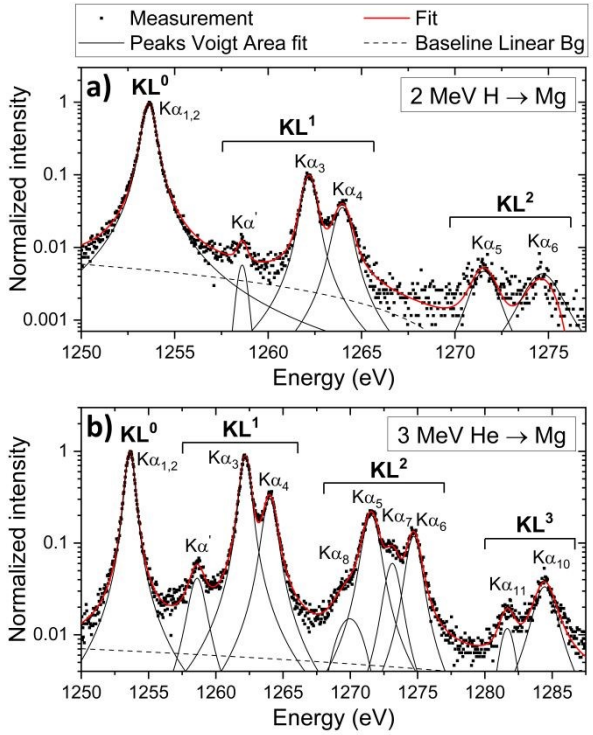

Figure 2. Fitted Kα X-ray emission spectra of Mg excited by a) 2 MeV H and b) 3 MeV He, normalized with respect to the KL^0 line. Spectra include all peaks' components and linear background.

View Article Online
DOI: 10.1039/D5JA00382B

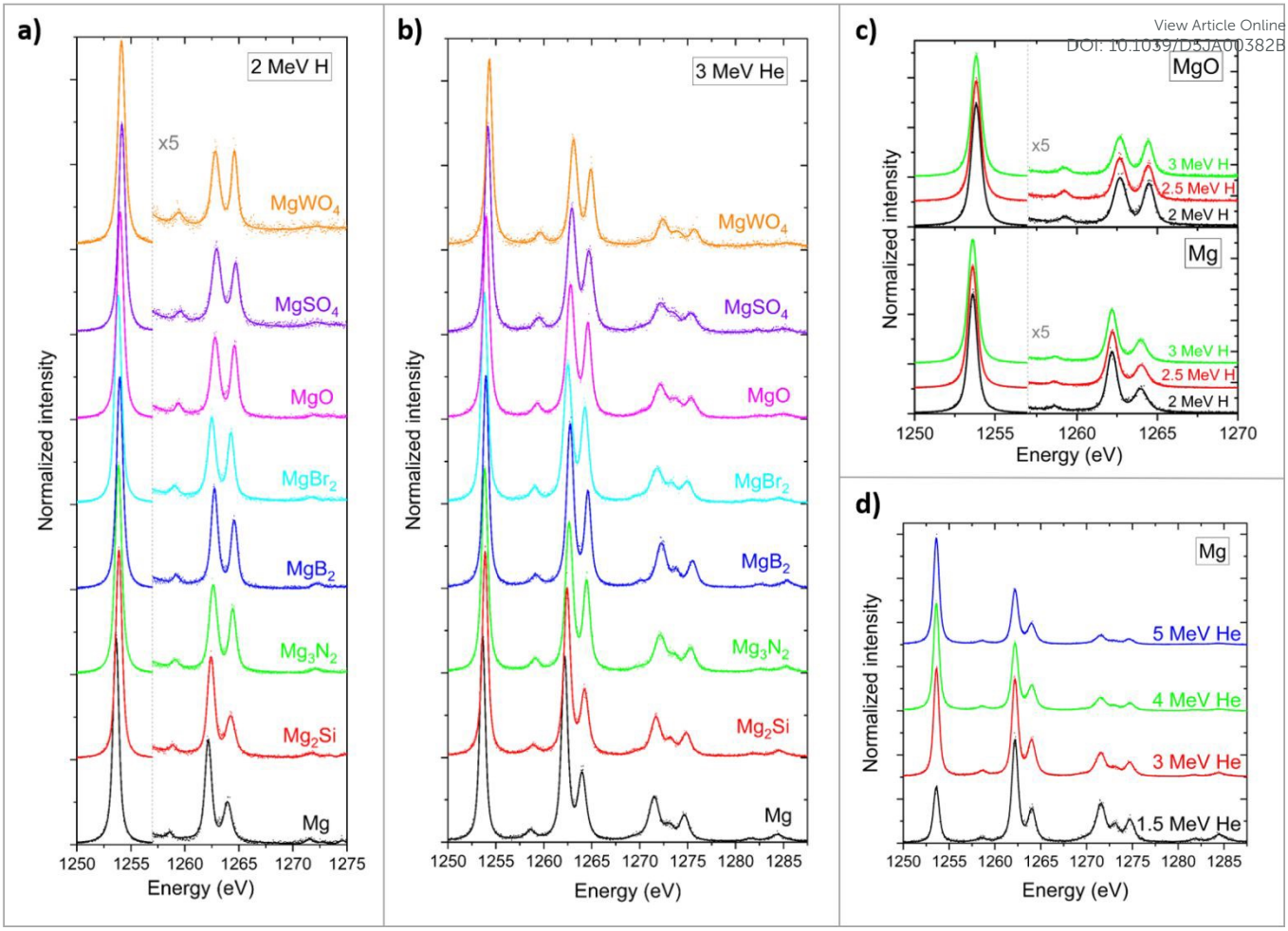

Figure 3. Fitted Kα X-ray emission spectra of Mg and its selected compound excited by a) 2 MeV H and b) 3 MeV He. c) Fitted Kα X-ray emission spectra of Mg and MgO excited by H beam at three different energies: 2, 2.5 and 3 MeV. d) Fitted Kα X-ray emission spectra of Mg excited by He beam at four different energies: 1.5, 3, 4 and 5 MeV. The intensities of spectral regions containing MIS lines in a) and c) are multiplied by a factor of 5 for plotting purposes. All spectra are normalized to their maximum intensity.

using the Voigt function – a convolution of the Gaussian instrumental profile and the Lorentzian X-ray line shape. Only the initial value of the Gaussian width, as previously determined in Ref.[10], was defined. The parameter was then allowed to vary freely during the fitting process, along with all other peak parameters (area, center and Lorentzian width). A linear background was included, which provided a suitable approximation given the narrow energy range. Figure 2 presents two examples of fitted spectra, together with all their components, for both 2 MeV H and 3 MeV He irradiation. As previously noted, MISs are more pronounced under He excitation, resulting in a larger number of resolved Kα lines.

Results and discussion

The calibrated and corrected Kα X-ray spectra, together with their corresponding fits, for Mg and its compounds irradiated with 2 MeV H and 3 MeV He are presented in Figures 3a and 3b. In addition, Figure 3c shows spectra related to Mg and MgO targets irradiated with 2, 2.5, and 3 MeV H, while Figure 3d displays spectra for Mg metal target irradiated with 1.5, 3, 4, and 5 MeV He.

Energy shifts

Figure 4 presents the energy shifts of the $K\alpha_{1,2}$ and $K\alpha_3$ lines in measured Mg compounds relative to pure Mg determined from 2 MeV H-induced X-ray spectra. The only previously reported energy shifts found in the literature are for MgO, measured by Fischer et al.[17] for 10 keV electron excitation, which are also plotted in Figure 4. Our measured energy shifts align well with Ref.[17] values, differing by 13% for $K\alpha_{1,2}$ and 7% for $K\alpha_3$.

These energy shifts arise from changes in valence electron density of an atom inside a compound, which reduce the effective nuclear potential experienced by its core electrons. As such, measuring these shifts should provide insight into the effective charge on Mg atoms within the solid and they do not depend on the atom's excitation mode.

For previously studied third-row elements, such as P, S, Cl and Al,[18,9] a negative linear correlation has been observed between $K\alpha_1$ energy shifts and calculated effective charges on the investigated atoms. It is reasonable to assume a similar relationship holds for Mg $K\alpha_{1,2}$ energy shifts. Accordingly, similar energy shifts within different compounds suggest a similar effective charge on Mg atoms in those compounds. It is worth noting the similarity in the measured $K\alpha_{1,2}$ energy shifts

View Article Online
DOI: 10.1039/D5JA00382B

Table 2. Energy shifts of the Kα4, Kα5 and Kα6 lines in measured Mg compounds relative to pure Mg. For comparison, the corresponding energy shifts reported in Ref. [17] for electron excitation are also included.

Compound	Energy shift (eV)						
	Kα4 2 MeV H	Kα4 3 MeV He	Kα4 10 keV e	Kα5 3 MeV He	Kα5 10 keV e	Kα6 3 MeV He	Kα6 10 keV e
$MgBr_2$	0.25±0.06	0.26±0.05		0.3±0.1		0.1±0.1	
Mg_2Si	0.31±0.05	0.31±0.05		0.22±0.09		0.2±0.1	
Mg_3N_2	0.54±0.04	0.54±0.04		0.70±0.09		0.6±0.1	
MgO	0.60±0.05	0.57±0.05	0.55 [17]	0.6±0.1	0.5 [17]	0.7±0.1	0.3 [17]
MgB_2	0.65±0.04	0.68±0.05		0.79±0.09		0.9±0.1	
$MgSO_4$	0.72±0.06	0.73±0.05		0.70±0.09		0.7±0.1	
$MgWO_4$	0.75±0.05	0.85±0.05		0.9±0.1		1.0±0.1	

for $MgSO_4$ and $MgWO_4$, which is consistent with the fact that Mg is bound to tetrahedral XO_4^{2-} anions in both compounds. Also, this implies a trend in which the effective charge decreases from pure Mg toward the more oxidized compounds on the x-axis of Figure 4, ending with $MgSO_4$ and $MgWO_4$.

The Kα1,2 and Kα3 energy shifts were uniquely determined from 2 MeV H-induced X-ray spectra related to the selected mixtures of Mg compounds and Ge. In contrast, the energy shifts of the Kα4 line were extracted from X-ray spectra of pure Mg compounds induced by both 2 MeV H and 3 MeV He. These values are listed in Table 2, together with the values for MgO from Ref.[17]. As expected, the two excitation modes yield consistent results. The average energy shift of the MgO Kα4 line agrees well with the results from Ref.[17], differing by 7%.

Table 2 also presents the energy shifts of the Kα5 and Kα6 lines. These were determined solely from X-ray spectra induced by 3 MeV He, where these MISs are clearly visible. The measured MgO energy shifts deviate from Ref.[17] values by 20% for Kα5 and 133% for Kα6.The large deviation observed for the Kα6 shift may be attributed to the lower energy resolution of Ref.[17] spectra, as shown in Figure 3 of Ref.[17], where KL^2 group resolves only two peaks (Kα5 and Kα6). Figure 3b of this work clearly shows four resolved peaks (Kα5, Kα6, Kα7 and Kα8) for both Mg and MgO, which enables a more accurate determination of peaks' centroids.

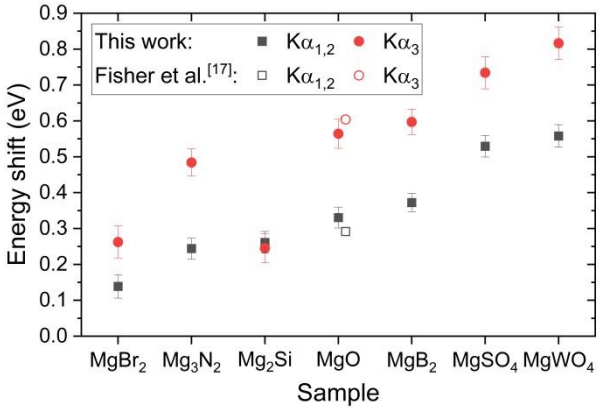

Figure 4. Energy shift of the Kα1,2 and Kα3 lines in measured Mg compounds relative to pure Mg. Filled symbols represent shifts measured in this study, while open symbols represent shifts reported in Ref.[17] for comparison.

Peak intensities

Figure 5 shows the relative intensity ratios of KL^1 to KL^0 for measured combinations of Mg targets and H ion beam energies. The intensity of each KL^n group was calculated as the sum of individual fitted peak areas within each group (see Figure 2). The shown uncertainties were calculated from statistical errors, as the square root of the number of counts within each KL^n group.

Irradiation with H ion beam did not result in significant variation in the relative KL^1 intensities across the different Mg compounds. For 2 MeV H excitation, the KL^1-to-KL^0 intensity ratios of different Mg targets differ from the average ratio by less than 5%. These differences could be explained by thick target self-absorption of Mg Kα X-rays.

With increasing H ion beam energy from 2 to 3 MeV, a downward trend in the KL^1-to-KL^0 intensity ratio was observed. Specifically, an energy increase from 2 to 2.5 MeV resulted in a ratio decrease of 8% for Mg and 10% for MgO. For further energy increase to 3 MeV, the ratio decreased by 18% for Mg and 14% for MgO. This behaviour reflects the dependence of inner-shell ionization cross sections on the ion beam energy.

Figure 6 shows the relative intensity ratio of KL^1 and KL^2 to KL^0 for measured combinations of Mg targets and He ion beam energies, alongside with the related intensity ratios reported by Heirwegh et al.[19] for Mg and MgO excited by He beams of similar energies.

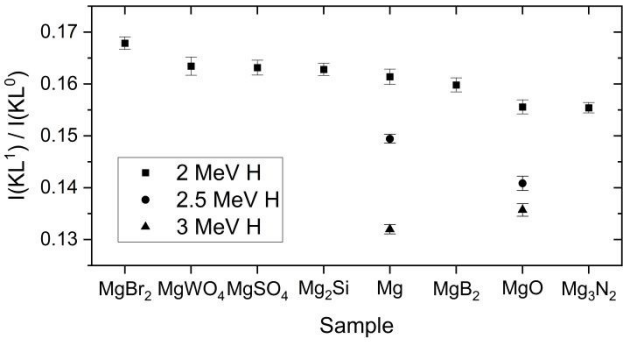

Figure 5. Intensity ratio of KL^1 to KL^0 X-ray emission lines of Mg and its compounds excited by H beam.

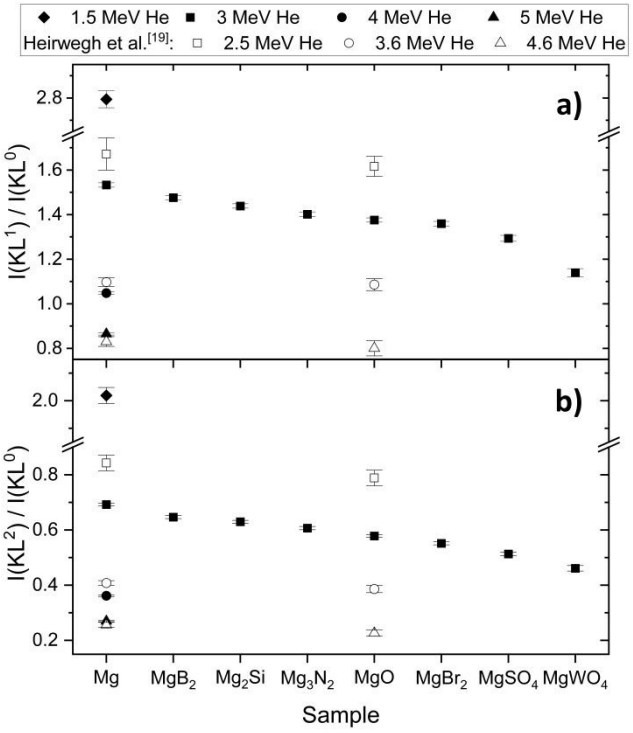

Figure 6. Intensity ratio of a) KL^1 to KL^0 and b) KL^2 to KL^0 X-ray emission lines of Mg and its compounds excited by He beam. Filled symbols represent measured ratios, while open symbols represent values reported in Ref.[19] for comparison.

3 MeV He excitation led to more observable variations in the relative KL^1 and KL^2 intensities across different Mg compounds. The KL^1-to-KL^0 ratios of Mg and $MgWO_4$ differ from the average ratio by 11% and 17% respectively, while differences for the other compounds remain below 8%. For the KL^2-to-KL^0 ratios, Mg and $MgWO_4$ differ from the average ratio by 18% and 21%, while the remaining compounds show differences of up to 13%. Determining whether these variations are influenced by chemical effects is not straightforward. However, the major source of the differences is probably the combined influence of thick-target self-absorption of Mg Kα X-rays and the higher stopping power of He ions compared with H ions. Because the relative intensities of MIS lines depend on ion energy, the measured spectrum represents a superposition of spectral contributions from all ion energies along its path in the target. For He excitation this ion-energy-loss effect is likely more pronounced than for H excitation.

In agreement with H excitation results, a strong negative correlation was found between He ion beam energy and the relative KL^1 and KL^2 intensities of metallic Mg. Specifically, an energy increase from 1.5 to 3 MeV resulted in the KL^1-to-KL^0 ratio decrease of 45%. For further energy increase to 4 MeV the ratio decreased by 63%, and at 5 MeV it decreased by 69%. The KL^2-to-KL^0 ratio decreased by 66% between 1.5 and 3 MeV, by 82% at 4 MeV, and by 87% at 5 MeV.

In Table 3, the KL^1-to-KL^0 intensity ratios for Mg and MgO excited by H and He ion beams are compared with corresponding ratios obtained for X-ray and electron excitation reported in the literature.[17,19-24] For H excitation in the 2 to 3 MeV energy range, the relative KL^1 satellite intensities fall within a similar range as those observed for X-ray and electron excitation.

Table 3. Intensity ratio of KL^1 to KL^0 X-ray emission lines of Mg and MgO. Bold values represent the present measurement, while non-bold values correspond to literature data reported in Refs. [17,19-24] for comparison.

Excitation		I(KL¹)/I(KL⁰) Mg	MgO
He ion beam	**1.5 MeV**	**2.79±0.04**	
	2.5 MeV[19]	1.67±0.07	1.62±0.05
	3 MeV	**1.53±0.01**	**1.38±0.01**
	3.6 MeV[19]	1.10±0.02	1.09±0.03
	4 MeV	**1.048±0.006**	
	4.6 MeV[19]	0.83±0.02	0.80±0.03
	5 MeV	**0.865±0.005**	
H ion beam	**2 MeV**	**0.161±0.001**	**0.156±0.001**
	2.5 MeV	**0.1494±0.0008**	**0.141±0.001**
	3 MeV	**0.1320±0.0009**	**0.136±0.001**
X-rays	Cr K[21]	0.140±0.003	0.158±0.002
	Rh L[22]	0.139±0.006	
	Cr K[23]	0.114±0.001	
electrons	4-5 keV[17]	0.161±0.005	0.159±0.005
	6 keV[24]	0.155±0.003	
	12 keV[20]	0.161±0.007	

In contrast to KL^1-to-KL^0 and KL^2-to-KL^0 ratios, the relative intensities of X-ray emission lines within the same group are not expected to be affected by thick target self-absorption, but only by chemical effects. Within the KL^1 group, clear differences in the relative intensities of the $K\alpha_3$ and $K\alpha_4$ lines, which are separated by less than 2 eV, are evident across different Mg targets in the measured spectra. It can be seen in Figures 3a and 3b that the increase in the $K\alpha_4$ intensity in going from Mg metal to Mg oxides is accompanied by a decrease in the $K\alpha_3$ intensity. These differences are illustrated in Figure 7, which presents the $K\alpha_4$-to-$K\alpha_3$ intensity ratios for both 2 MeV H and 3 MeV He excitation. The intensities and associated uncertainties of $K\alpha_3$ and $K\alpha_4$ peaks were derived from the fitted peak areas.

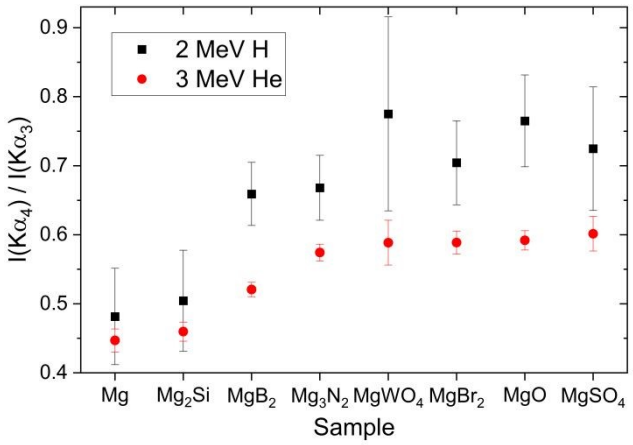

Figure 7. Intensity ratio of $K\alpha_4$ to $K\alpha_3$ X-ray emission lines of Mg and its compounds excited by H and He ion beams.

View Article Online
DOI: 10.1039/D5JA00382B

Differences in $K\alpha_4$-to-$K\alpha_3$ intensity ratios for metal and its compounds when excited by light ions are in previous works[25-27] attributed to the effect of Coster-Kronig transitions before the emission of Kα X-ray. Such transitions convert states that can deexcite via $K\alpha_4$ emission to states that can deexcite via $K\alpha_3$ emission. It has been proposed that Coster-Kronig transitions are available completely for a metal but are available to a lesser extent in compounds due to ionic binding energy. Our measurements agree with that interpretation. As shown in Figure 7, there is a clear difference in $K\alpha_4$ to $K\alpha_3$ intensity ratios for Mg metal and all measured compounds, except for Mg_2Si. The similarity in this ratio between Mg and Mg_2Si could be explained by the significant covalent character of the Mg–Si chemical bond. A review of the literature reveals that X-ray Photoelectron Spectroscopy (XPS) data indicate that Mg–Si bond in Mg_2Si is far from purely ionic (i.e. in which Mg valence electrons are entirely transferred to Si). In fact, its ionicity is only 8%.[28] Under 3 MeV He excitation, where the intensities of the $K\alpha_3$ and $K\alpha_4$ peaks could be measured with higher precision, a statistically significant deviation in the $K\alpha_4$-to-$K\alpha_3$ intensity ratio was also observed for MgB_2 compared to the other compounds. Literature data[29] suggest that the Mg–B bond is likewise not purely ionic, but has a substantial metallic (delocalized) electron contribution. These results demonstrate that examining the $K\alpha_4$-to-$K\alpha_3$ intensity ratio via WD PIXE spectrometry, particularly under He excitation, can provide insight into the nature of chemical bonding in the measured compound.

Figure 8 shows how $K\alpha_4$-to-$K\alpha_3$ intensity ratio varies with H and He ion beam energy. In addition to the measured data, the figure includes relevant values reported in the literature.[19,25,27] No statistically significant difference was observed in the measured $K\alpha_4$-to-$K\alpha_3$ intensity ratios for the H ion beam across the 2–3 MeV energy range. However, the measured ratios are lower than the corresponding literature values, by 16% for Mg and 22% for MgO. This discrepancy is likely due to differences in the methods used to determine peak areas.

Similarly, for the He ion beam in the 3–5 MeV range, the ratio remains largely unchanged. In this energy interval, the average of measured ratios is 10% higher than the literature values reported for 2.5-5.4 MeV. However, when the He beam energy is reduced to 1.5 MeV, the ratio drops significantly, by 17% compared with the average value at higher energies. A possible explanation lies in the larger variations between double K-L^i ionization cross sections at lower He beam energies, close to 1 MeV, compared with higher energies between 2-5 MeV used in this work.

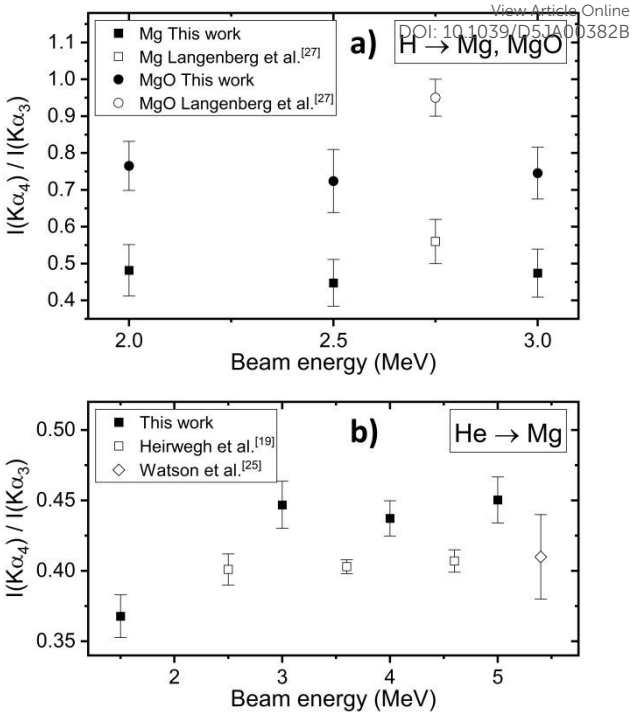

Figure 8. Intensity ratio of $K\alpha_4$ to $K\alpha_3$ X-ray emission lines of: a) Mg and MgO excited by H beam, and b) Mg excited by He beam. Filled symbols represent ratios measured in this study, while open symbols represent values reported in Refs.[19,25,27] for comparison.

Summary and conclusions

In this work, high-resolution WD X-ray emission spectra of the Mg Kα band were systematically investigated in metallic Mg and a series of Mg compounds excited by H and He ion beams of various MeV energies. The study focused on two aspects: the influence of chemical bonding and the effects of ion beam type and energy on the Mg Kα spectral line components. These aspects were examined through peak energy shifts and relative intensities of specific MIS lines within the overall spectral profile.

The Mg Kα X-ray spectra exhibit statistically significant variations in peak positions depending on the measured compound. The energy shifts of $K\alpha_{1,2}$ and MIS peaks among selected Mg compounds relative to metallic Mg are all less than 1 eV, yet remain measurable. Based on previous findings, we suggest that the relationship between $K\alpha_{1,2}$ shifts provides insight into the effective charge on Mg atoms in these compounds. Nevertheless, verifying this relationship in future studies would be valuable. In addition, analysis of the relative $K\alpha_4$ peak position in spectra induced by both 2 MeV H and 3 MeV He confirmed that the two excitation modes yield consistent results.

For 2-3 MeV H ion beam excitation, only KL^1 MIS group could be measured, with a KL^1-to-KL^0 intensity ratio of about 15%, showing a slight negative correlation with ion beam energy. In contrast, for 1.5-5 MeV He ion beam excitation, both KL^1 and KL^2 MIS groups were observed. The KL^1-to-KL^0 and KL^2-to-KL^0 intensity ratios varied strongly with He ion beam energy, ranging from 279% to 87% and from 202% to 27%, respectively. Measured trends reflect the dependence of inner-shell ionization cross sections on the ion beam type and energy.

Selected Mg compounds irradiated with 2 MeV H showed no significant variation in the KL^1-to-KL^0 intensity ratios. Small differences observed could be attributed to thick target self-absorption of Mg Kα X-rays. Observed variations in the KL^1-to-KL^0 and KL^2-to-KL^0 intensity ratios for 3 MeV He excitation were

more noticeable. It remains challenging to determine whether these differences come from chemical effects or are primarily due to enhanced ion-beam-energy-loss and related X-ray self-absorption in thick targets.

Statistically significant variations were observed in the relative intensities of the KL[1] group components. The $K\alpha_4$-to-$K\alpha_3$ intensity ratios, measured for both 2 MeV H and 3 MeV He excitation, showed a strong dependence on the chemical bonding within the target. Since MIS components are more pronounced with 3 MeV He excitation, it allows chemical speciation via the $K\alpha_4$-to-$K\alpha_3$ intensity ratio with higher precision compared to H excitation. Changes in ion beam energy produced no statistically significant differences in the measured $K\alpha_4$-to-$K\alpha_3$ intensity ratios for H beam in the 2–3 MeV range nor for He beam in the 3–5 MeV range. In contrast, the ratio decreased remarkably when the He beam energy was reduced to 1.5 MeV.

The results of this study confirm that PIXE performed with a WD spectrometer having adequate energy resolution can be efficiently used to study chemical effects in Kα X-ray band of Mg using H and He ion beams in MeV energy range. Also, this work will contribute to constructing a more extensive and accurate database of MIS X-ray lines for H and He ions, which is needed to improve fitting and interpretation of standard ED X-ray spectra in PIXE analysis software.

Conflicts of interest

There are no conflicts to declare.

Acknowledgements

AM, IBM, SF and MRR acknowledge the support from the Croatian Science Foundation project Hi-REXS [Grant Number 9429].

References

1 B. Schmidt and K. Wetzig, *Ion Beams in Materials Processing and Analysis*, Springer, 1st edn., 2013.
2 Y. Wang and M. Nastasi, *Handbook of Modern Ion Beam Materials Analysis*, Materials Research Society, 2nd edn., 2009, vol. 2.
3 S. Fazinić, I. Božičević-Mihalić, G. Provatas, T. Tadić, M. Rubel, E. Fortuna-Zaleśna and A. Widdowson, *Nucl. Fusion*, 2020, **60**, 126031.
4 L. Beck, in *X-Ray Spectrometry*, John Wiley and Sons Ltd, 2005, **34**, 393–399.
5 D. J. T. Cureatz, M. Kavčič, M. Petric, K. Isaković, I. B. Mihalić, M. R. Ramos, S. Fazinić and J. L. Campbell, *Spectrochim. Acta, Part B*, 2022, **194**, 106483.
6 J. L. Campbell, D. J. T. Cureatz, E. L. Flannigan, C. M. Heirwegh, J. A. Maxwell, J. L. Russell and S. M. Taylor, *Nucl. Instrum. Methods Phys. Res., Sect. B*, 2021, **499**, 77–88.
7 C. M. Heirwegh, J. L. Campbell and G. K. Czamanske, *Nucl. Instrum. Methods Phys. Res., Sect. B*, 2016, **366**, 40–50.
8 Y. Ito, T. Tochio, M. Yamashita, S. Fukushima, T. Shoji, K. Słabkowska, Ł. Syrocki, M. Polasik, J. P. Gomilsek, J. P. Marques, J. M. Sampaio, M. Guerra, J. Machado, J. P. Santos, A. Hamidani, A. Kahoul, P. Indelicato and F. Parente, *Int. J. Mol. Sci.*, 2023, **24**, 5570.
9 S. Fazinić, I. B. Mihalić, A. Mioković, M. R. Ramos and M. Petric, *J. Anal. At. Spectrom.*, 2023, **38**, 2179–2187.
10 I. Božičević Mihalić, A. Mioković, M. Rodriguez Ramos, D. Cosic, D. Mudronja, M. Tkalčević and S. Fazinić, *Measurement (Lond)*, 2024, **238**, 115325.
11 I. B. Mihalić, S. Fazinić, T. Tadić, D. Cosic and M. Jakšić, *J. Anal. At. Spectrom.*, 2016, **31**, 2293–2304.
12 S. Fazinić, I. Božičević Mihalić, T. Tadić, D. Cosic, M. Jakšić and D. Mudronja, *Nucl. Instrum. Methods Phys. Res., Sect. B* Elsevier B.V., 2015, **363**, 61–65.
13 R. D. Deslattes, E. G. Kessler, P. Indelicato, L. De Billy, E. Lindroth and J. Anton, *Rev. Mod. Phys.*, 2003, **75**, 35–99.
14 H. S. Kainth, *J. Alloys Compd.*, 2019, **782**, 404-412.
15 S. Lafuerza, A. Carlantuono, M. Retegan and P. Glatzel, *Inorg. Chem.*, 2020, **59**, 12518–12535.
16 A. Iwata, K. Yuge and J. Kawai, *X-Ray Spectrom.*, 2013, **42**, 16–18.
17 D. W. Fischer and W. L. Baun, *Spectrochim. Acta*, 1965, **21**, 448–450.
18 M. Petric and M. Kavčič, *J. Anal. At. Spectrom.*, 2016, **31**, 450–457.
19 C. M. Heirwegh, M. Petric, S. Fazinić, M. Kavčič, I. B. Mihalić, J. Schneider, I. Zamboni and J. L. Campbell, *Nucl. Instrum. Methods Phys. Res., Sect. B*, 2018, **428**, 9–16.
20 E. Mikkola, O. Keski-Rahkonen, J. Lahtinen and K. Reinikainen, *Phys. Scr.*, 1983, **28**, 188–192.
21 J. Utriainen, M. Linkoaho, E. Rantavuori, T. Aberg and G. Graeffe, *Zeitschrift fur Naturforschung A*, 1968, **23**, 1178–1182.
22 K. Parthasaradhi, G. R. Babu, V. Radha, K. Murty, M. V. R. Murti and K. S. Rao, *Nucl. Instrum. Methods Phys. Res., Sect. A*, 1987, **255**, 54-55.
23 O. Mauron, J.-C. Dousse, J. Hoszowska, J. P. Marques, F. Parente and M. Polasik, *Phys. Rev. A*, 2000, **62**, 062508.
24 M. O. Krause and J. G. Ferreira, *J. Phys. B:At., Mol. Opt. Phys.*, 1975, **8**, 2007-2014.
25 R. L. Watson, A. Langenberg and F. E. Jenson, *Jpn. J. Appl. Phys.*, 1978, **17**, 93–96.
26 V. Radha Krishna Murty, V. Gopalakrishna, M. L. N. Raju, B. Mallikarjuna Rao, K. Parthasaradhi, M. V. R. Murti and K. S. Rao, *Phys. Rev. A*, 1988, **38**, 2171–2173.
27 A. Langenberg and R. L. Watson, *Phys. Rev. A*, 1981, **23**, 1177–1187.
28 Z. Fan, H. N. Ho, R. Szczęsny, W. R. Liu and D. H. Gregory, *CrystEngComm*, 2022, **24**, 5801–5809.
29 J. M. Osorio-Guillén, S. I. Simak, Y. Wang, B. Johansson and R. Ahuja, *Solid State Commun.*, 2002, **123**, 257–262.

View Article Online
DOI: 10.1039/D5JA00382B

Data for this article are available at Fulir DATA Ruđer Bošković Institute Research Data Repository at https://data.fulir.irb.hr/.